

# **An Alternative Algorithm for the Calculation of Primary Productivity from Remote Sensing Data**

by  
**John Marra  
Cheng Ho  
Charles C. Trees\***

**LDEO Technical Report**

**# LDEO-2003-1**

**National Aeronautics and Space Administration  
Grant #  
NAG5-11215**

**February 3, 2003**

**Lamont-Doherty Earth Observatory  
of Columbia University  
and  
\*Center for Hydrologic Optics and Remote Sensing, San Diego State  
University**

Approved for public release: distribution unlimited

## Abstract

An algorithm for the calculation of primary productivity from space is presented. The algorithm is based on irradiance, the absorption of irradiance by phytoplankton, and the efficiency with which that irradiance is converted to fixed carbon. The absorption of irradiance by phytoplankton is discussed based on recent measurements from the Sargasso Sea, the boreal North Atlantic, the Southern Ocean, and the Arabian Sea. It is found that the chlorophyll-specific absorption coefficient varies in a predictable way with sea-surface temperature, and this can be used to parameterize an optical characteristic of phytoplankton as a function of geographic location and season. The photosynthetic conversion efficiency (quantum yield), however, is more difficult to parameterize. Because of the variability of its maximum value, choosing a maximum quantum yield is a limitation of the algorithm at present. Other algorithms are examined for their ability to predict *in situ* primary productivity, using data from the Arabian Sea. Although the comparisons in this report are limited, these other algorithms fail to predict *in situ* productivity.

## Table of Contents

<b>INTRODUCTION</b>	5
<b>THE ALGORITHM</b>	5
1. Phytoplankton Absorption Coefficient	6
2. Quantum Efficiency of Photosynthesis	9
<b>RESULTS</b>	10
1. PPARR3	10
2. The influence of mixed layer depth on this algorithm	11
3. Computation of $P(z)$ from $P_{vsE}$	17
5. Comparison with B&F in terms of integral PP	19
<b>DISCUSSION</b>	20
<b>REFERENCES</b>	22
<b>APPENDIX 1</b>	24

## List of Figures

- Fig. 1. The chlorophyll-specific absorption coefficient ( $a^*_{ph}$ )(0-5 m) as a function of sea-surface temperature for a variety of investigations. The lines are best fits to the data for temperatures above 12 C. Below 12 C,  $a^*_{ph}$  is assumed to be constant. The PS pigment line assumes that 85% of the absorption is from photosynthetic pigments (see text).
- Fig. 2. Primary production calculated using Equation (1) and measured in situ for three different programs in the North Atlantic Ocean.
- Fig. 3 (a) Output of the algorithm presented in this document for the PPARR3. The months begin with January 1998 (9801). The total global productivity for each month in Gigatons C (“GT C/month”) is identified. These results are also available at <ftp://oceans-www.jpl.nasa.gov/pub/mec/>
- Fig. 3 (b) Same as Fig. 3a, but for the algorithm “Behrenfeld” (Behrenfeld and Falkowski, 1997).
- Fig. 4 (a) Log-log plot of primary production from the algorithm against mixed layer depth for 7 months in 1998 (98mm) in the Atlantic Ocean. The correlation coefficients are also given in each panel.  
(b) Same as Fig. 4(a) but for 7 months in 1998 in the Pacific Ocean.  
(c) Same as Fig. 4(a) but for 7 months in 1998 in the Indian Ocean. The correlation coefficients are also given in each panel.
- Fig. 5. Primary productivity for cruise TN045 of the Arabian Sea Program, as a function of depth, and as measured in situ (open symbols) and as predicted from PvsE relationships, also measured the same day.
- Fig. 6. Primary productivity for selected stations during the Arabian Sea Program, as estimated by the model of Behrenfeld and Falkowski (1997) and as measured in situ. The closed symbols are productivity measurements for dawn-to-dusk incubations and the open symbols are incubations from dawn to dawn.

## INTRODUCTION

In 1995, we participated in the first Primary Productivity Working Group inter-comparison of algorithms to estimate ocean productivity from space. That effort, called the Primary Production Algorithm Round-Robin 1 (PPAR1) culminated in a publication, now in press (Campbell et al., 2002). A major conclusion was that the algorithms were about equal in explaining the variance in the data, despite having marked differences in the sophistication of the models. For example, very simple models, based only on mixed layer depths and a value for the maximum photosynthesis did about as well as models that calculated depth-resolved productivity at each wavelength.

Probably because it was published first, and was easy to employ, the algorithm of Behrenfeld and Falkowski (1997a; Hereafter, BF97) has become standard in many investigations. We were motivated, however, by two major factors. First, we felt the need for an algorithm more coupled to the optical properties in the surface layer, so that as knowledge of the inherent optical properties of the ocean improved, it would lead to improvements in our ability to calculate productivity. Also, changes in, for example, solar input would be coupled to the output of the model. Second, the algorithm should allow for physiological adaptation in the phytoplankton. We were also motivated by the moderate success we have had in the past in using the basic formula for the algorithm in calculating primary production as a function of depth from phytoplankton absorption and irradiance (Marra et al., 1992, Marra et al., 1993; Marra et al., 1995).

The algorithm in its present state is by no means perfect, and is in many respects oversimplified. It is presented in the hopes of inspiring further research into the absorption properties of the ocean, and in understanding the environmental influences on photosynthetic quantum efficiencies in the phytoplankton.

## THE ALGORITHM

The algorithm is based on the equation first used by Bannister (1974) and Kiefer and Mitchell (1983). Daily primary production,  $P$ , at depth  $z$  can be written,

$$P(z) = \Phi \cdot a_{ph} \cdot E(z), \quad (1)$$

where  $\Phi$  is the quantum yield ( $\text{mol C mol photons}^{-1}$ ),  $a_{ph}$  is the absorption coefficient of the phytoplankton ( $\text{m}^{-1}$ ), and  $E(z)$  is the irradiance ( $\text{mol photons m}^{-2} \text{d}^{-1}$ ). Equation (1) is interesting in that it doesn't require the determination of chlorophyll. However, in the case of the PPARR, chlorophyll is supplied as an input variable. Also, irradiance is given as photosynthetically active radiation (PAR), which is the total flux of photons between wavelengths of 400-700 nm.

Thus, we use the chlorophyll-specific phytoplankton absorption coefficient,  $a_{ph}^*$ , and PAR irradiance,

$$P(z) = \Phi \cdot a_{ph}^* \cdot Chla \cdot E_{par}(z), \quad (2)$$

where Chla is the quantity of chlorophyll-a ( $\text{mg m}^{-3}$ ), and  $a_{ph}^*$  has the units  $\text{m}^2 (\text{mg Chla})^{-1}$ . The two inputs to the model are Chlorophyll-a and  $E_{par}(z)$ . These can be supplied through measurements on shipboard, or from satellite observations (see the SeaWiFS homepage, <http://seawifs.gsfc.nasa.gov> for available data products). Eq. (2) does not fit clearly with the types of models discussed in Behrenfeld and Falkowski (1997b). It is not a wavelength-resolved model (WRM), nor is it a vertically-integrated model (VIM). Thus, for Equation (2), we need to supply values for the absorption coefficient and the quantum yield. In previous studies from shipboard,  $a_{ph}$  was measured, and Eq. (2) was only applied locally. Using satellite data, assigning values to  $a_{ph}$  and  $\Phi$  means deriving functions that reproduce the geographic or temporal variability in these model variables, functions that are little known. We now deal with phytoplankton absorption and quantum efficiencies in turn.

### 1. Phytoplankton Absorption Coefficient

The primary determinants to the phytoplankton absorption coefficient are (1) pigment composition, and (2) the 'package' effect. The first factor is obvious. Each pigment has a characteristic absorption spectrum, which will be reflected in the overall absorption in the cell. The package effect refers to the difference (decrease) in absorption resulting from the fact that phytoplankton pigments are not dissolved, but occur in chloroplasts, or packages, within the cell. There are conflicting reports about the importance of the package effect in natural populations (Allali et al., 1997; Marra et al., 1997; Bissett et al., 1997). The package effect is determined not only by the fact that pigments are not in solution, but packaged, but because of the size and shape of the cells as well. Increasing the size and extending the shape will increase the package effect. Smaller cells are less likely to exhibit the package effect since pigments occupy a greater percentage of the cellular space than in large cells. The size spectrum of phytoplankton is thought to change with productivity. Productivity generally is a function of latitude, although there are well-known and conspicuous exceptions near the equator and in low-latitude upwelling regimes near coastlines. But we can expect to find, proportionally, larger cells in less stable environments (Malone, 1980), and which are often found at higher latitudes, and smaller cells in more stable environments, such as, the tropics. Phytoplankton pigments can be divided into three major groupings: (1) those that participate directly in photochemical energy conversion, such as chlorophyll-a, (2) those that transfer photons to the chlorophyll-a (e.g. the photosynthetic carotenoids), and those that help protect the chloroplasts from an excess of irradiance, and called the photoprotectant carotenoids. Thus another driver in phytoplankton absorption is the determinants of the pigment composition of the phytoplankton.

For PPARR1, we had relatively little phytoplankton absorption data on which to base a functional relationship that would extend beyond the local measurements. However, we did have seasonal values of  $a^*_{ph}$  from the site of the mooring in the North Sargasso Sea during the Biowatt-2 program (see Marra et al., 1992), and those were used to generate a spatially-generalized, seasonally-dependent  $a^*_{ph}$  used in the algorithm (see Campbell et al., 2002). The other feature of the distribution of  $a^*_{ph}$  is its lack of dependence on depth. We have found a lack of depth dependence in Biowatt-2, the Marine Light-Mixed Layers program (see Marra et al., 1993, Marra et al., 1995), the Arabian Sea Expedition (Marra et al., 2000; Johnson et al., 2002) and in the AESOPS program (Vaillancourt et al., 2002). Sosik and Mitchell (1995) failed to find a depth-dependence in the CalCOFI area. Depth-dependence does not seem to be universal, however. Allali et al. (1997) and Dupouy et al. (1998) both found a depth dependence of  $a^*_{ph}$  in the tropical Pacific. We will assume for the time being, that  $a^*_{ph}$  does not vary with depth in the euphotic zone. In the data of Allali et al. (1997),  $a^*_{ph}$  does not vary significantly within the top two optical depths.

For PPARR3, we had the advantage of many more observations of phytoplankton absorption, and spanning a wider geographic range. And what we needed was a mechanism to allow for the geographic and spatial variability of  $a^*_{ph}$ , but which was not dependent, at least directly, on the other inputs to the algorithm. Since sea-surface temperature (SST) is available globally from satellite, and is independent of chlorophyll (at least), we plotted the near-surface values of  $a^*_{ph}$  against SST. The resulting relationship is shown in Figure 1. Overall, the relationship is not bad, but it is difficult to fit a standard function to the entire data set. An exponential fit, for example, would underestimate the values near 0°C. Higher order fits would introduce unwarranted curvature into the relationship. Thus, for below 12°C, we used a straight-line fit to the lowest temperature observations of  $a^*_{ph}$ .

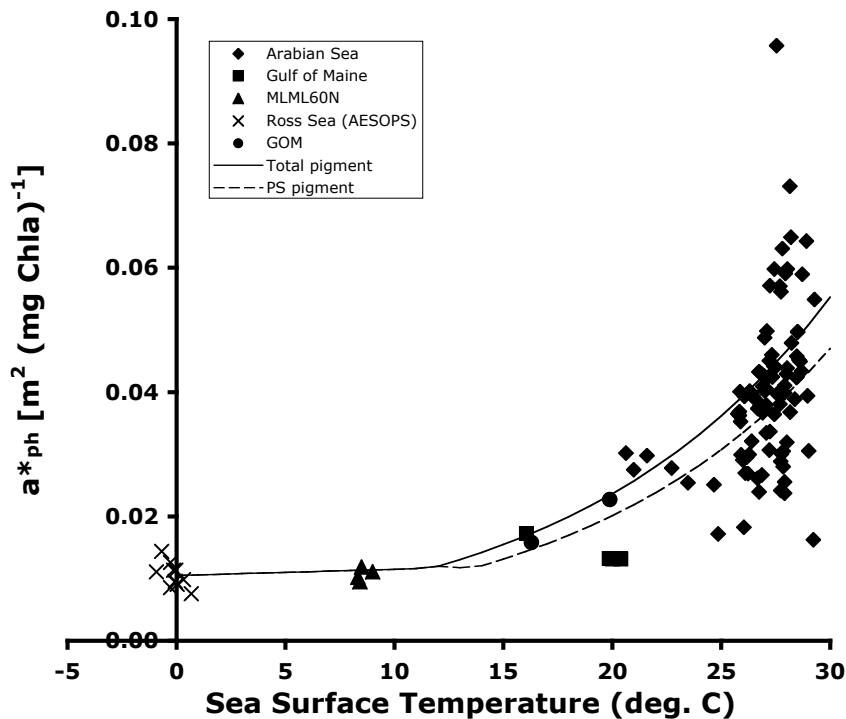


Fig. 1. The chlorophyll-specific absorption coefficient ( $a^*_{ph}$ )(0-5 m) as a function of sea-surface temperature for a variety of investigations. The lines are best fits to the data for temperatures above 12 C. Below 12 C,  $a^*_{ph}$  is assumed to be constant. The PS pigment line assumes that 85% of the absorption is from photosynthetic pigments (see text).

It is important to remember that the fit in Fig. 1 is largely operational. It is not based on phytoplankton physiology, for example. Sosik and Mitchell (1994), one of the only studies we are aware of where  $a^*_{ph}$  was examined as a function of phytoplankton growth at various temperatures in culture, found that  $a^*_{ph}$  would decrease with increasing temperature of growth. The relationship instead is based on phytoplankton community structure. Generally speaking, warmer SSTs are associated with lower latitudes where there are more stable water columns, and nutrient-depleted conditions. This has been termed the 'Typical Tropical Structure' by Herbland and Voituriez(1979). The possible exception is in upwelling regimes, especially in places like Indonesia and the Arabian Sea, where upwelled water remains above 23°C.

The trend in Fig. 1 follows the trend in plots of  $a^*_{ph}$  against chlorophyll-a, such as in Bricaud et al. (1995), and also the analysis of Cleveland (1995). Those analyses show  $a^*_{ph}$  to be a declining function of the quantity of chlorophyll-a, perhaps to be expected if a normalized value is plotted against what it is normalized to. Plotting a random number against its inverse will always result in a declining exponential relationship, much like that found in Bricaud et al. (1995). Chlorophyll-a in Bricaud et al. (1995) has the double function of being a biomass

indicator as well as an indicator of trophic conditions of the ocean, something we avoid here.

We have found for the Arabian Sea, that photoprotectant pigments cause a significant part of the absorption, and this is probably true in other tropical and sub-tropical areas. Thus, we have also shown a line that tries to capture that part of the variability in  $a^*_{ph}$ . Photoprotectant pigments seem to be a minor contribution to phytoplankton absorption, or else absent, in polar regions (R.R. Bidigare, personal communication). For the purposes of the algorithm here, we assume that photoprotectant pigments would cause a reduction in  $a^*_{ph}$  by 15%.

## 2. Quantum Efficiency of Photosynthesis

Quantum efficiency can either be influenced by irradiance or nutrients, depending on which is more limiting, and can be written as a Michaelis-Menten dependence (Kiefer and Mitchell, 1983). Thus, for irradiance dependence,

$$\square = \square_{max} [(K_m + E(z))/K_m], \quad (3)$$

Where  $\square_{max}$  is a maximum value for the quantum efficiency, and  $K_m$  is the irradiance where  $\square$  reaches half its maximum value. Eq. (3) was a good description of the rate of primary production in Biowatt-2 (Marra et al., 1992), and in the first cruise of the Marine Light-Mixed Layers program (Marra et al., 1993). However, Bidigare et al. (1992) recommended the use of a hyperbolic tangent relationship as a better fit to the data,

$$\square = \square_{max} \tanh(K_e/E(z)) \quad (4)$$

Where  $K_e$  is now a constant analogous to the  $E_k$  in the PvsE response curve. Eq. (4) was subsequently adopted for the Arabian Sea (Marra et al., 1998, Marra et al., 2000).

The difficulty in using either of the above equations is that they introduce two new variables to the calculation of primary productivity from chlorophyll-a and irradiance,  $\square_{max}$  and  $K_b$ . The highest observed value of  $\square_{max}$  is  $0.125 \text{ mols O}_2 (\text{mols photons})^{-1}$ , however it is not a constant (e.g., Cleveland et al., 1989), and will be less than the historical maximum because of respiration losses, other metabolic demands, and because the rates are measured in terms of carbon rather than oxygen. A reasonable estimate for the growth time scale of phytoplankton would be 0.06, or about half the highest observed value. A further problem with  $\square$  is that it cannot be measured directly, that is, without recourse to the absorption coefficient.

For the algorithm, therefore, and until we understand the environmental drivers for its variability, we are forced to choose a value for  $\square_{max}$ . For tests in the North Atlantic of Equation (1) as a predictor of  $P(z)$ , a value of 0.06 for  $\square_{max}$  and a  $K_e$  of

10 mol photons  $m^{-2} d^{-1}$  explained most of the data (Fig. 2). However, for the Arabian Sea, a  $\mu_{max}$  of 0.03-0.04 was more appropriate. This range of values also agrees with the results from the PvsE response curves, calculating  $\mu_{max}$  from the product of the initial slope of the curve ( $\mu$ ) and  $a^*_{ph}$ . (However, see below.) We assume that  $K_e$  remains constant at 10 mol photons  $m^{-2} d^{-1}$ .

The algorithm, as a Matlab file, is in Appendix 1.

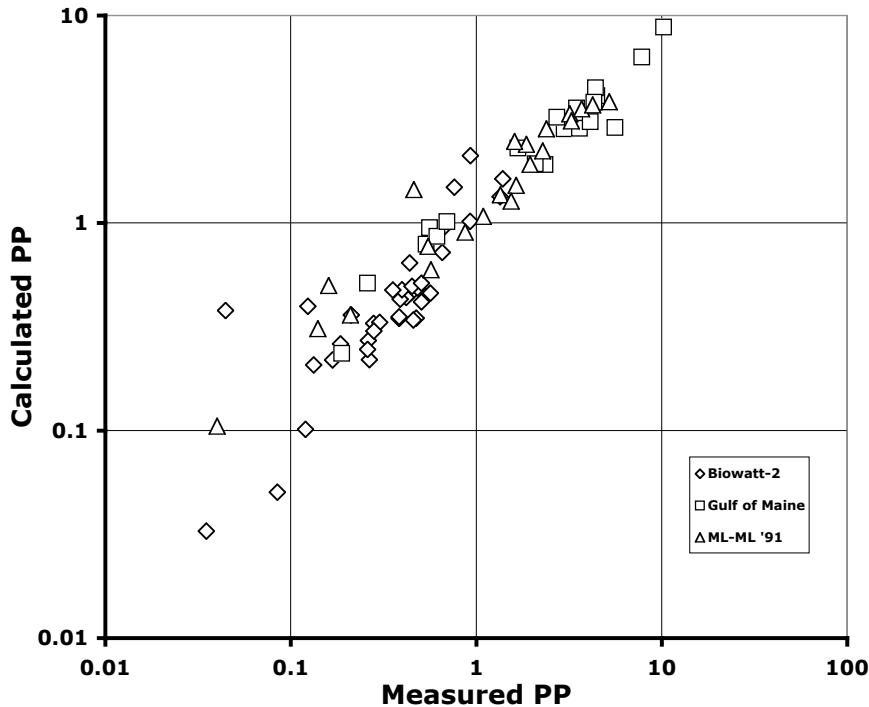


Fig. 2. Primary production calculated using Equation (1) and measured in situ for three different programs in the North Atlantic Ocean.

## RESULTS

### 1. PPARR3

For PPARR3, each investigator was given global SeaWiFS chlorophyll and surface PAR data for 7 monthly periods in 1998: January, March, May, July, September, November, and December. The results are available from the Mary-Elena Carr at JPL at <http://oceans-www.jpl.nasa.gov/pub/mec/>. A few of those plots are reproduced here.

Given that the data are comparative only, we compare the output of our algorithm with the de facto standard, Behrenfeld and Falkowski (1997), as produced here in their standard output. (M. Behrenfeld submitted two formulations of his model to PPARR3.) Fig. 3 shows results from the “Very Generalized Productivity Model” (VGPM) of Behrenfeld and Falkowski (1997) (Fig 3a, “Behrenfeld”), and the algorithm presented here (Fig. 3b, “Marra”). The results from both differ mostly in the contrasts between so-called oligotrophic and eutrophic areas of the ocean. Another overall difference is that the seasonal increases in both the South and North Atlantic occur earlier in Behrenfeld than in “Marra”. The “Behrenfeld” algorithm has higher productivity in austral spring than in “Marra”, and the bloom off eastern South America occurs earlier in the growing season. The spring bloom in the North Atlantic appears to begin in January or March in “Behrenfeld”, but is stronger in “Marra”. The “Marra” algorithm is higher in the Indian Ocean than the “Behrenfeld” algorithm, especially in Southeast Asia. There are differences, as well, in the Arabian Sea.

## 2. The influence of mixed layer depth on this algorithm

Mixed layer depths were provided during PPARR3 from the Levitus atlas and NCAR. Some algorithms use the mixed layer depth as an input into the calculation (see Campbell et al., 2002), using data on the mixed layer depth from Levitus and Boyer (1994). We wanted to see if the results from our algorithm were correlated with the mixed layer depth. The results from that analysis are shown in Fig. 4. In very few cases was primary production positively correlated with mixed layer depth, which is expected if stability and irradiance are the important factors. The weak negative correlations are probably significant, given the number of data points. But the coefficient of determination will also be low, which means that the mixed layer depth is explaining very little of the variability in the productivity data. For the Atlantic, during some months (January, May and November, for example), mixed layer depth appears to set an upper limit, but nothing more. We conclude, that for our algorithm, mixed layer depth is not a significant factor in determining productivity from space.

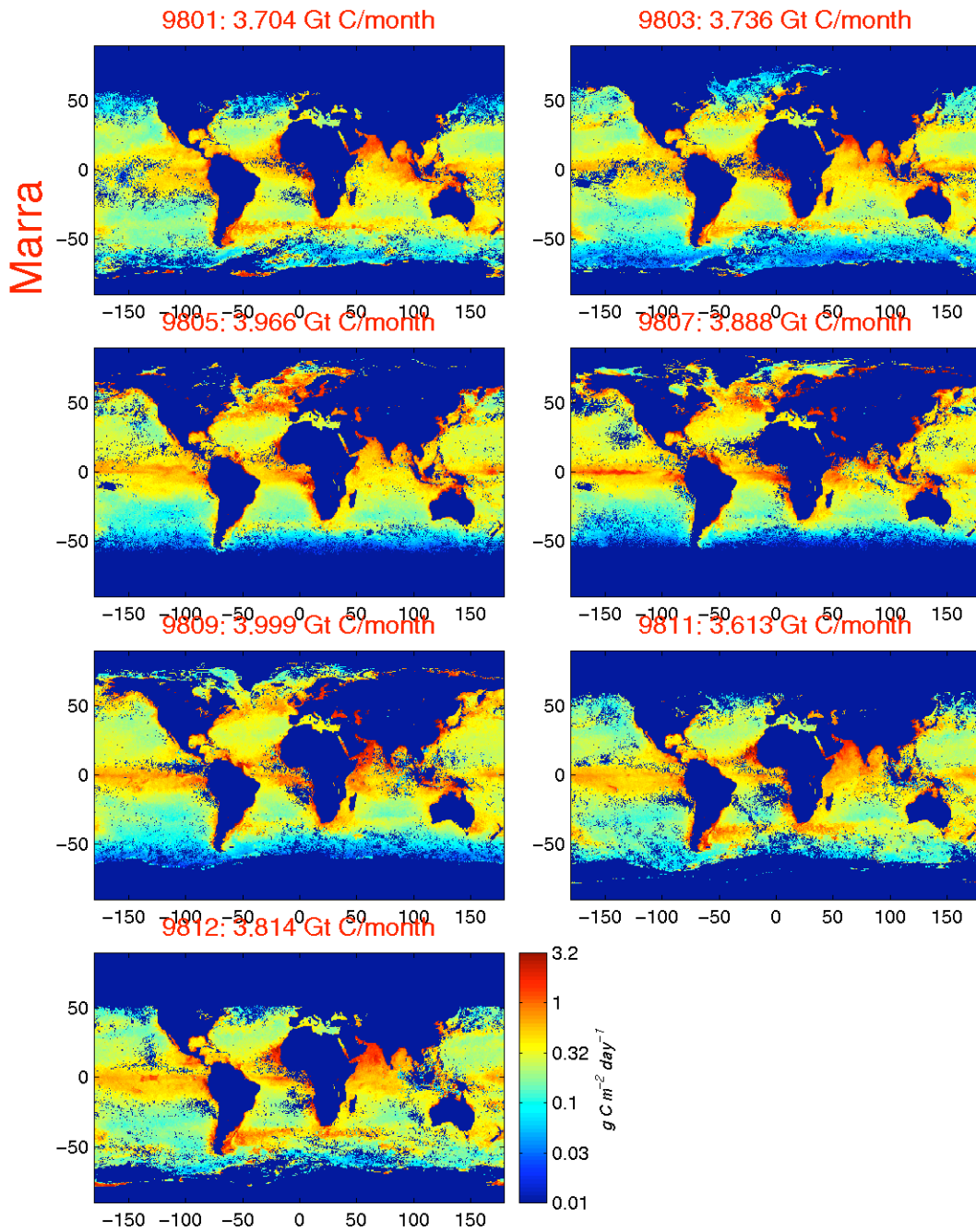


Fig. 3(a). Output of the algorithm presented in this document for the PPARR3. The months begin with January 1998 (9801). The total global productivity for each month in Gigatons C (“GT C/month”) is identified. These results are also available at <http://oceans-www.jpl.nasa.gov/pub/mec/>

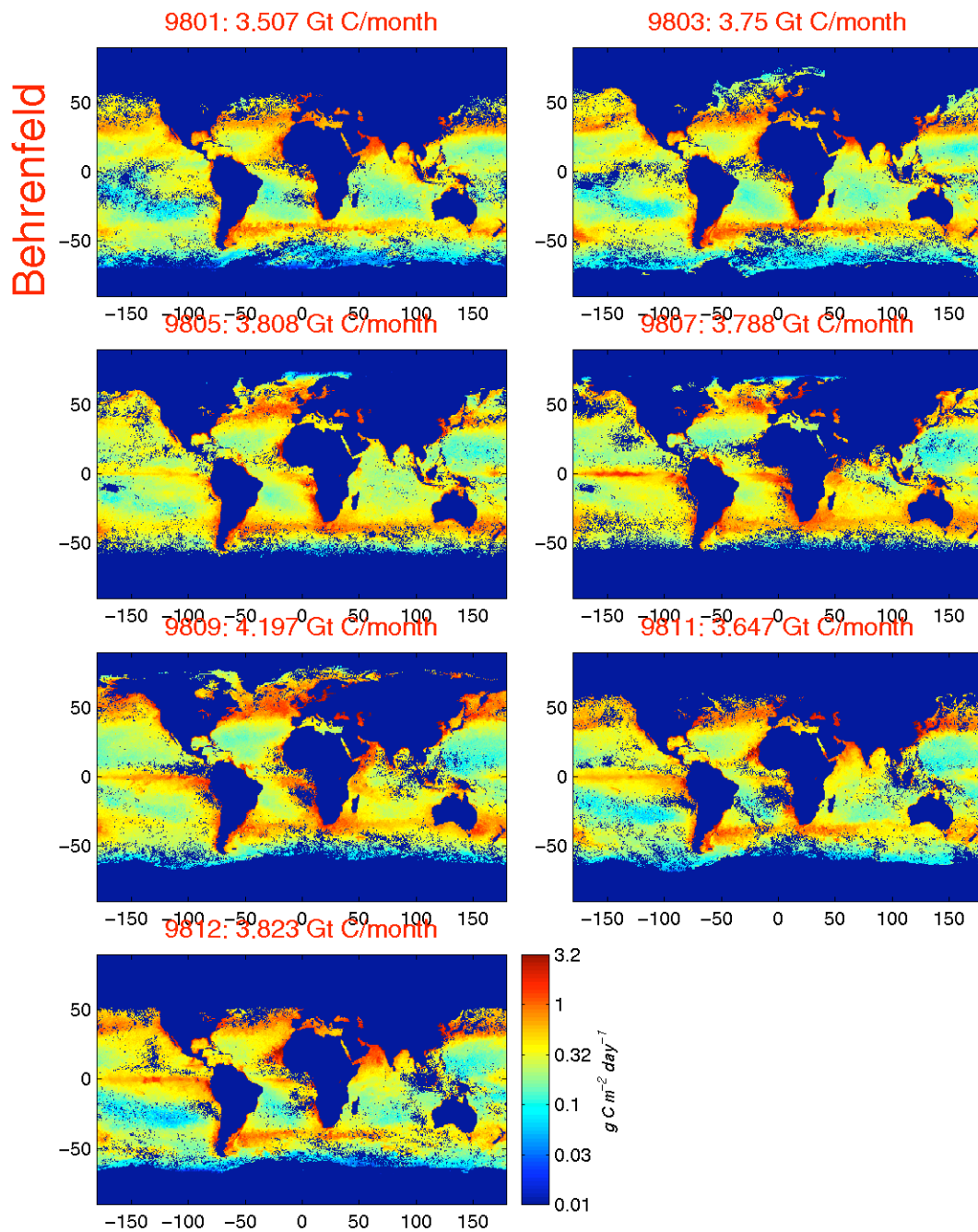


Fig. 3(b). Same as Fig. 3a, but for the algorithm “Behrenfeld” (Behrenfeld and Falkowski, 1997).

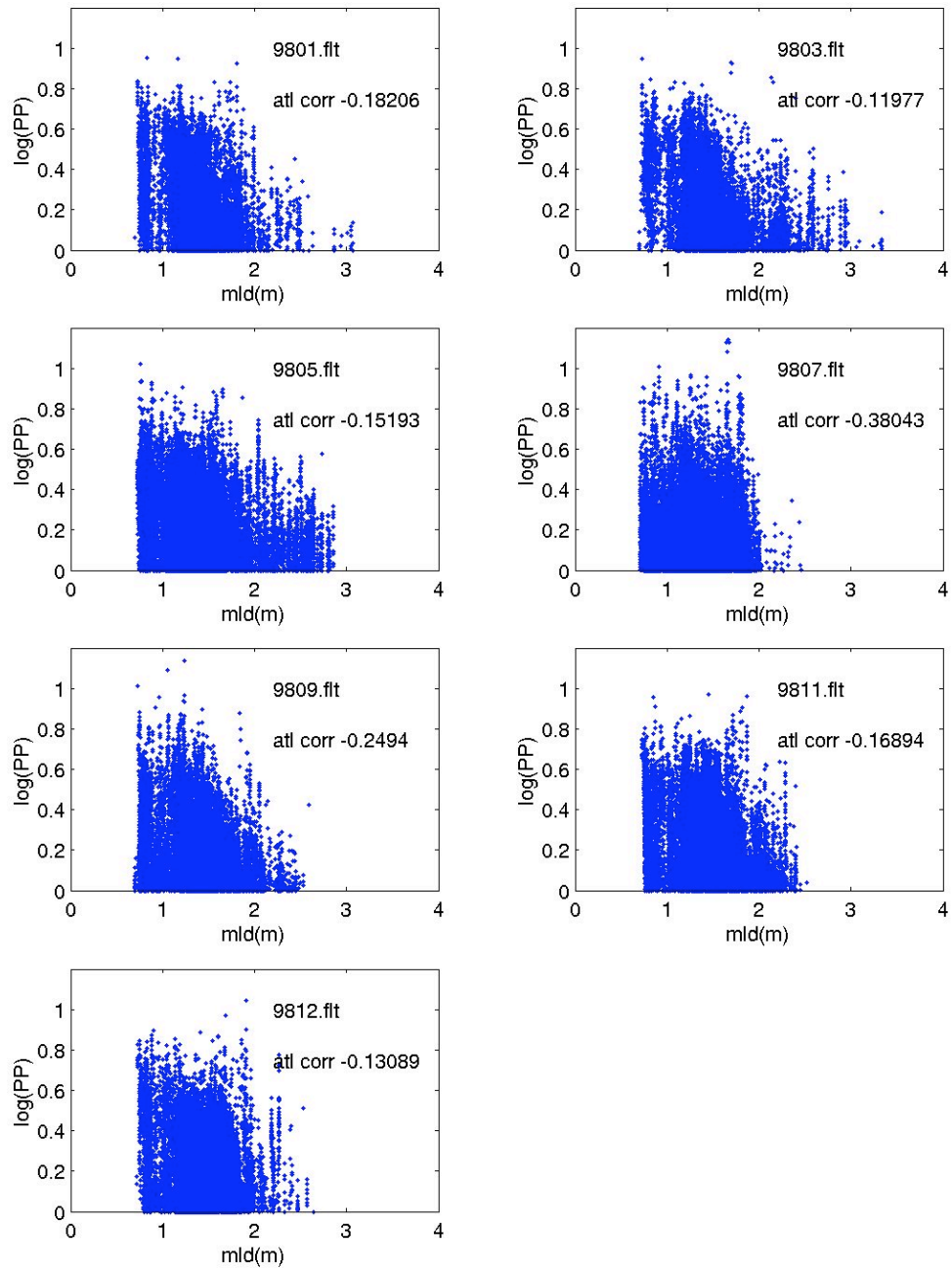


Fig. 4 (a) Log-log plot of primary production from the algorithm against mixed layer depth for 7 months in 1998 (98mm) in the Atlantic Ocean. The correlation coefficients are also given in each panel.

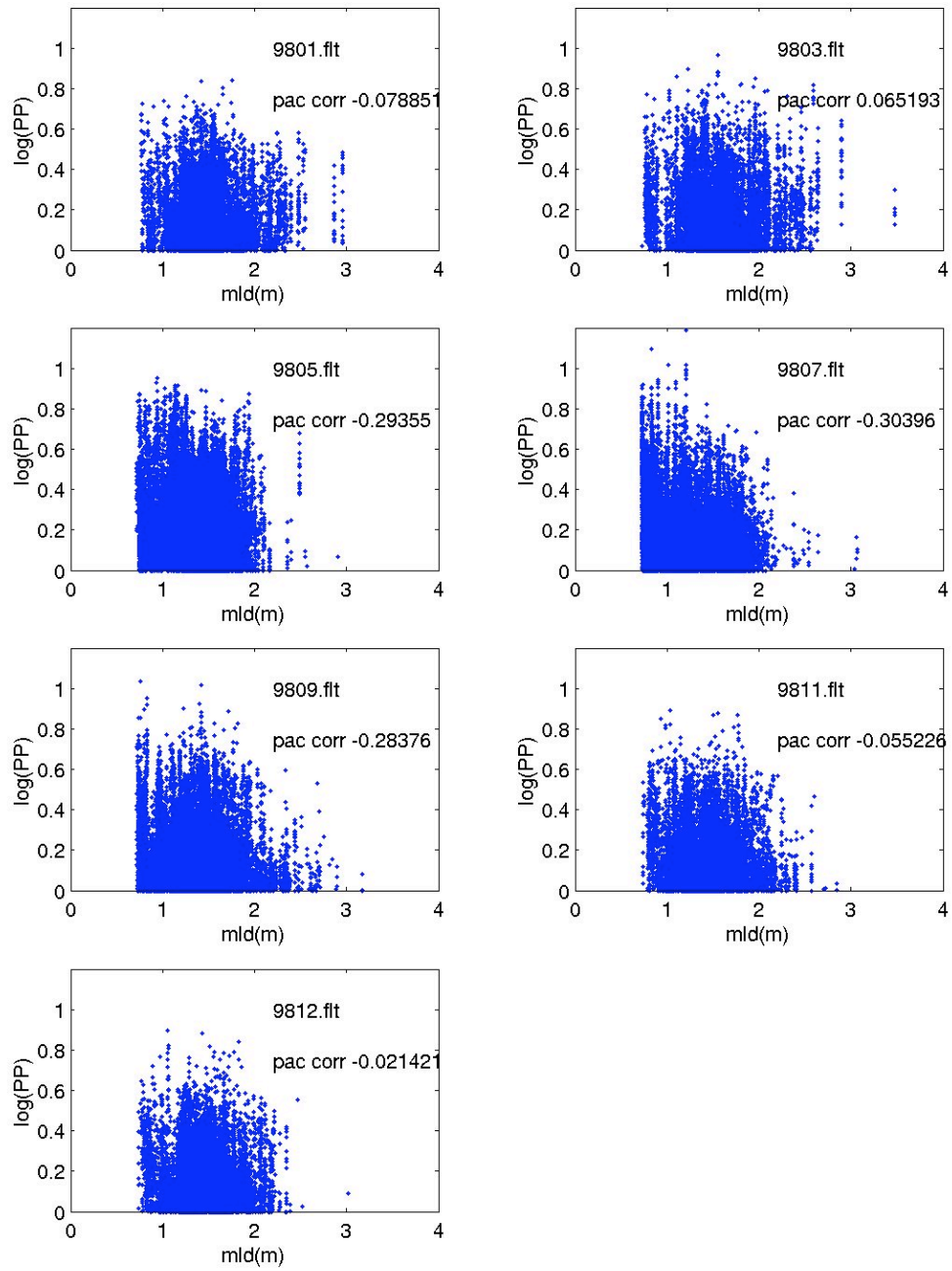


Fig. 4 (b) Same as Fig. 4(a) but for 7 months in 1998 in the Pacific Ocean.

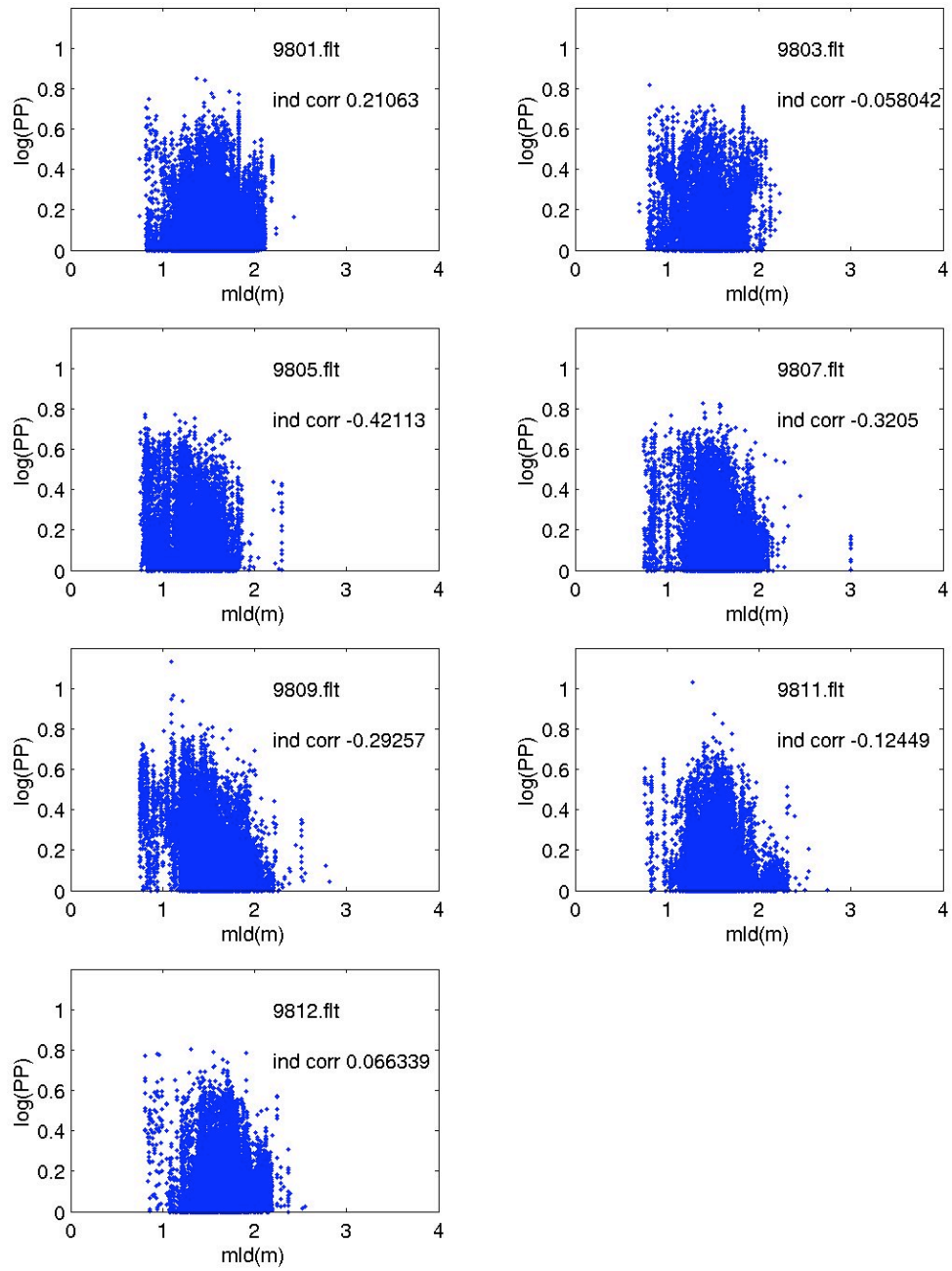


Fig. 4 (c) Same as Fig. 4(a) but for 7 months in 1998 in the Indian Ocean. The correlation coefficients are also given in each panel.

### 3. Computation of P(z) from PvsE

A typical means of calculating primary production from remote sensing data is by means of the photosynthesis versus irradiance (PvsE) response (e.g., Platt et al., 1980). The resulting curve can be defined in terms of two or three parameters (e.g., Jassby and Platt, 1976, Platt et al., 1980), but more typically two, the initial slope and the maximum rate. The magnitude of the initial slope, called  $\alpha$ , is an indication of the efficiency of photosynthesis, because of the linear relationship with irradiance. The maximum, called  $P_{max}$ , is an indication of the limitations caused by, for example, the dark reactions, or carbon fixation pathways. In a typical form (Jassby and Platt, 1976),

$$P(t,z) = P_{max}(t,z) \cdot \tanh (\alpha(t,z) \cdot E(t,z)/P_{max}(t,z)). \quad (5)$$

Depending on the times and depths of the determinations of  $\alpha$  and  $P_{max}$ ,  $P$  is then integrated over the day and the euphotic zone to achieve a daily, areal rate of primary production,

$$PP = \iint P(t,z) dt \cdot dz$$

The largest assumption underscoring Eq. (5) is that  $P_{max}$  and  $\alpha$  are constant as a function of depth or time such that the integrations can be an accurate reflection of PP. If diel variations are thought to be important, more frequent PvsE determinations can be made, and the time integral limits established for shorter time periods. Likewise, we can expect significant depth variability in  $\alpha$  and  $P_{max}$ , and thus we have to know how appropriately to integrate Eq. (5) as a function of depth. Thus, there are two steps in the process (1) formulating the PvsE response and the parameters, and (2) integrating those over depth and time. Usually, the parameters are normalized to chlorophyll-a, which serves, in this case, as a measure of phytoplankton biomass.

There are not many tests of this method, that is, comparing the output of integrating a PvsE function with *in situ* measurements of primary production. Harrison et al. (1985) found differences in  $P(z)$  that they ascribed to possible artifacts from deck incubators (cf. Barber et al., 1997), but the areal rates between the two methods were the same, statistically. Harrison et al. (1985) cite several references where agreement had been found between calculations from PvsE parameters and measured rates of primary production. Cote and Platt (1984) also compared estimates based on PvsE parameters with *in situ* rates of carbon assimilation, however, only for the duration of each experiment. Such a comparison would validate the use of 'simulated' *in situ* methods, but would not predict day-length determinations of carbon assimilation.

We have made a similar comparison, using data from the Arabian Sea Expedition in 1995. During those cruises, PvsE experiments were conducted

around noon of the day in which *in situ* primary production measurements were made. To be sure, the measurements, while at the same location, were made on hydrocasts separated by about 6 h. The details of each method are in Marra et al. (2000), Barber et al. (2001), and Johnson et al. (2002). The *in situ* measurements of <sup>14</sup>C uptake were accompanied by *in situ* measurements of PAR irradiance as a function of time, providing estimates of E(t). There were typically three such sensors for each experiment, thus an estimate of the attenuation coefficient (Kz) as well as the irradiance just beneath the surface (Epar(0-)) was obtained for the day of the *in situ* productivity experiment. The PvsE experiments were done near noon, at 6 depths in the water column, and with an incubation time of 2 h.

To conform to the determinations of the PvsE experiments, Epar(0-) was averaged over each hour of the day, and primary production was calculated at each of the depths for which an experiment was performed, and used as follows,

$$P(t,z) = P_{\max}(z) \cdot \tanh\left(\frac{E(t,0-) \cdot \exp(-Kz \cdot z)}{P_{\max}(z)}\right)$$

Sample comparisons of depth-dependent primary production are shown in Fig. 5. As shown, the computation of daily P(z) from the PvsE parameters is about 50-75% less than that of the *in situ* measurements.

Aside from the differences in time, one source of error is the possible calibration differences between the *in situ* sensors and the PvsE incubators. If we assume the PvsE incubator irradiances are correct, and increase the *in situ* irradiances by a factor of two, that still does not account for the differences between the two methods. Another possibility would be growth in the incubation bottles *in situ*, causing an overestimate in the *in situ* measurement of production compared to the PvsE estimate. 'Bottle artifacts' of this kind are difficult to evaluate. Bender et al. (1999) concluded that growth in the bottles was occurring in the Equatorial Pacific for 24-h incubations. On-deck "grow-out" experiments usually have to be conducted over periods of 5-6 days for growth to be evaluated (e.g., Martin et al., 1991). For the North Atlantic Bloom Experiment (NABE), using techniques identical to those here, *in situ* incubations agreed with the draw-down of total CO<sub>2</sub> in the mixed layer (Chipman et al., 1993). One indication of a bottle effect is to measure chlorophyll-a before and after an incubation. But chlorophyll-a may increase or decrease caused by a variety of effects. Grazing or deleterious effects might produce a decrease; photoadaptation or cell growth might cause an increase. The point here is that if PvsE measurements were relied on exclusively, a different picture would arise of primary production in the Arabian Sea.

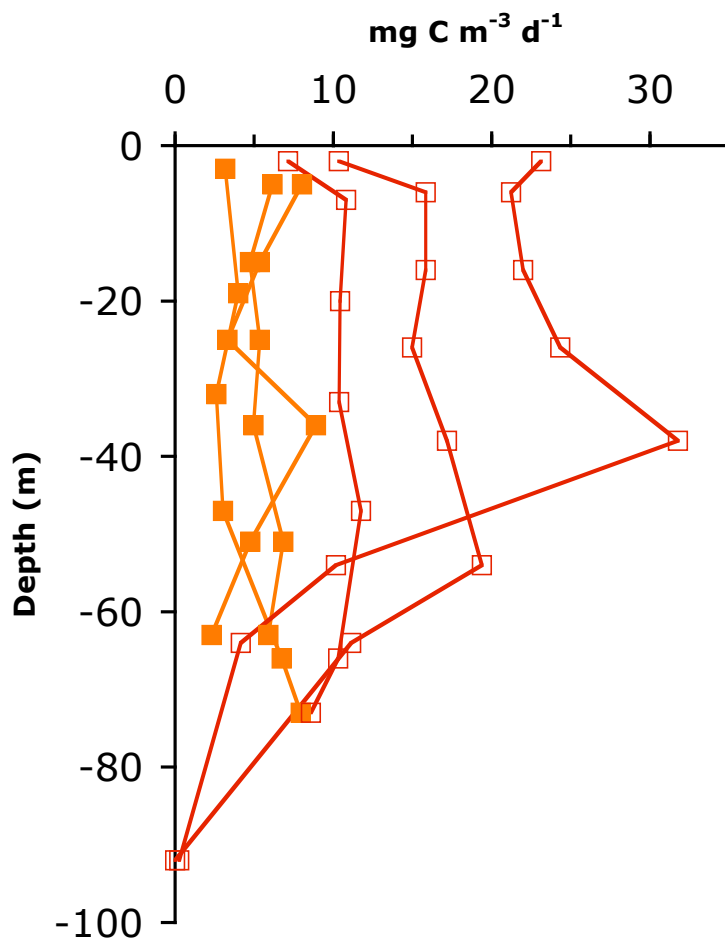


Fig. 5. Primary productivity for cruise TN045 of the Arabian Sea Program, as a function of depth, and as measured *in situ* (open symbols) and as predicted from PvsE relationships, also measured the same day (closed symbols).

### 5. Comparison with B&F in terms of integral PP

We have made some initial comparisons of our *in situ* primary production measurements from Biowatt-2 and the Arabian Sea with the output of the algorithm of Behrenfeld and Falkowski (1997). Recall that the algorithm presented here does well in predicting  $P(z)$  (Fig. 2). BF97 is a vertically-integrated model, thus the comparison involves an integral of the *in situ* data. The comparison is shown in Fig. 6. Although the data are in the same range, there is not a correlation between *in situ* productivity and the output of the algorithm in BF97. At this point, we have the opportunity to compare relatively few stations, however, based on these, the prognosis is not good for a satisfactory comparison of *in situ* primary production with the BF97 algorithm.

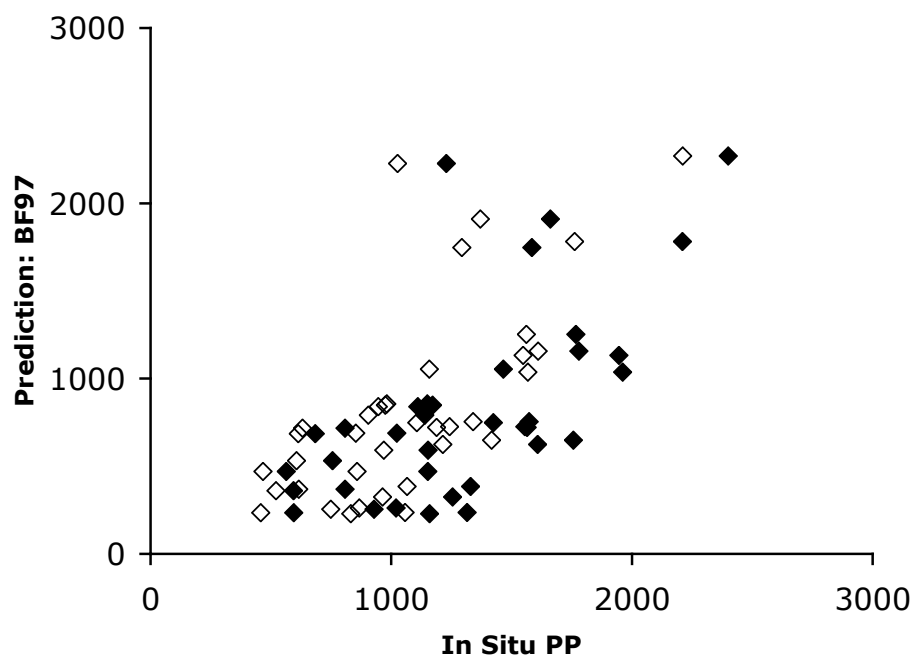


Fig. 6. Primary productivity for selected stations during the Arabian Sea Program, as estimated by the model of Behrenfeld and Falkowski (1997) and as measured *in situ*. Units are  $\text{mg C m}^{-2} \text{d}^{-1}$ . The closed symbols are productivity measurements for dawn-to-dusk incubations and the open symbols are incubations from dawn to dawn.

## DISCUSSION

The productivity algorithm here is promising but is in need of further work. For example, we need to understand more about how phytoplankton absorption varies with environmental properties. Relying on phytoplankton absorption in an algorithm means that we also need to be able to understand the variability in the absorption of other absorbing and scattering components of the ocean as well, such as that of pure water, colored dissolved organic matter (CDOM), and other particulate substances. In future, perhaps we can forget about chlorophyll-a, and just calculate absorption from the remote sensing reflectance directly. Chlorophyll-a, as used here, is more a convenience than anything else.

Similarly, we don't understand the variability in the quantum yield. We have a range of values that could be used for the maximum value. At least we know that quantum yield will be a saturating function of irradiance and nutrients, but we need better knowledge of the parameters of the curve. Unfortunately, we cannot estimate quantum yields of phytoplankton photosynthesis without recourse to the absorption coefficient. We need to devise a means for a non-absorption-based

estimate of the quantum yield, perhaps through measurements of fast-repetition-rate fluorometry (FRRF), or pulse-amplitude modulated (PAM) fluorometry. In the meantime, an understanding of the environmental determinants to quantum yields in phytoplankton would help in giving more geographic resolution to the model. We recommend that more attention be made on surveys of phytoplankton absorption rather than on surveys of the photosynthesis-response. Solutions to all of these problems are some time in the future, however the algorithm is promising enough that it can serve as a research agenda.

## REFERENCES

- Allali, K., A. Bricaud and H. Claustre (1997). Spatial variations in the chlorophyll-specific absorption coefficients of phytoplankton and photosynthetically active pigments in the equatorial Pacific. *Journal of Geophysical Research* 102(C6): 12413-12423.
- Bannister, T. T. (1974). Production equations in terms of chlorophyll concentration, quantum yield, and upper limit to production. *Limnology and Oceanography* 19: 1-12.
- Barber, R. T., L. Borden, Z. Johnson, J. Marra, C. Knudson, C.C Trees. (1997). Groundtruthing modeled kPAR and on deck primary productivity incubations with in situ observations. *Ocean Optics XIII*, Halifax, NS, SPIE.
- Barber, R.T., J. Marra, R.R. Bidigare, L.A. Codispoti, D. Halpern, Z. Johnson, M. Latasa, R. Goericke, S.L. Smith (2001) Primary productivity and its regulation in the Arabian Sea during 1995. *Deep-Sea Research II* 48, 1127-1172.
- Behrenfeld, M. J., and P.G. Falkowski (1997a). Photosynthetic rates derived from satellite-based chlorophyll concentration. *Limnology and Oceanography* 42(1): 1-20.
- Behrenfeld, M. J., and P.G. Falkowski (1997b). A consumer's guide to phytoplankton primary productivity models. *Limnology and Oceanography* 42(7): 1479-1491.
- Bender, M., J. Orchardo, M.-L. Dickson, R.T. Barber and S. Lindley. (1999). In vitro O<sub>2</sub> fluxes compared with <sup>14</sup>C production and other rate terms during the JGOFS Equatorial Pacific Experiment. *Deep-Sea Research* 46: 637-654.
- Bidigare, R. R., B.B. Prezelin, and R.C. Smith (1991). Bio-optical models and the problems of scaling. Primary productivity and biogeochemical cycles in the sea. P. G. F. a. A. D. Woodhead. New York, Plenum.
- Bissett, W. P., J.S. Patch, K.L. Carder and Lee, Z.P. (1997). Pigment packaging and Chl-a specific absorption in high-light oceanic waters. *Limnology and Oceanography* 42: 961-968.
- Bricaud, A., M. Babin, A. Morel, and H. Claustre (1995). Variability in the chlorophyll-specific absorption coefficients of natural phytoplankton: Analysis and parameterization. *Journal of Geophysical Research* 100(C7): 13321-13332.
- Campbell, J. W., D. Antoine, R. Armstrong, K. Arrigo, W. Balch, R. Barber, M. Behrenfeld, R. Bidigare, J. Bishop, M.-E. Carr, W. Esaias, P. Falkowski, N. Hoepffner, R. Iverson, D. Kiefer, S. Lohrenz, J. Marra, A. Morel, J. Ryan, V. Vedernikov, K. Waters, C. Yentsch, and J. Yoder (2002). Comparison of algorithms for estimating ocean primary productivity from surface chlorophyll, temperature, and irradiance. *Global Biogeochemical Cycles* 16(3), 10.1029/2001GB001444.
- Chipman, D. J. Marra and T. Takahashi (1993). Primary production at 47°N/20°W: A comparison between the <sup>14</sup>C incubation method and mixed layer carbon budget observations. *Deep-Sea Research II* 40: 151-169.
- Cleveland, J. S. (1995). Regional models for phytoplankton absorption as a function of chlorophyll a concentration. *Journal of Geophysical Research* 100(C7): 13333-13344.
- Cleveland, J. S., M.J. Perry, D.A. Kiefer, and M. C. Talbot (1989). Maximal quantum yield of photosynthesis in the northwestern Sargasso Sea. *Journal of Marine Research* 47: 869-886.
- Cote, B. and T. Platt (1984). Utility of the light-saturation curve as an operational model for quantifying the effects of environmental conditions on phytoplankton photosynthesis. *Marine Ecology-Progress Series* 18: 57-66.
- Dupouy, C., J. Neveux, and J. M. Andre (1998). Spectral absorption coefficient of photosynthetically active pigments in the equatorial Pacific Ocean (165E-150W). *Deep-Sea Research II* 44: 1881-1906.
- Harrison, W. G., T. Platt and M.R. Lewis. (1985). The utility of light-saturation models for estimating marine primary productivity in the field: a comparison with conventional "simulated" in situ methods. *Canadian Journal of Fisheries and Aquatic Sciences* 42: 864-872.
- Herbland, A. and B. Voituriez (1979). Hydrological structure analysis for estimating the primary production in the tropical Atlantic Ocean. *Journal of Marine Research* 37(87-101).

- Jassby, A. D. and T. Platt (1976). Mathematical formulation of the relationship between photosynthesis and light for phytoplankton. *Limnology and Oceanography* 21: 540-547.
- Johnson, Z., R.R. Bidigare, R. Goericke, J. Marra, C. Trees and R.T. Barber (2002) Photosynthetic physiology and physicochemical forcing in the Arabian Sea, 1995. *Deep-Sea Research II* 49, 415-436.
- Kiefer, D. A. and B.G. Mitchell (1983). A simple, steady state description of phytoplankton growth based on absorption cross section and quantum efficiency. *Limnology and Oceanography* 28: 770-776.
- Levitus S. and T.P. Boyer, 1994c, *World Ocean Atlas 1994, Volume4: Temperature*, NOAA Atlas NESDIS 4 11pp.
- Malone, T. C. (1980). Size-fractionated primary productivity of marine phytoplankton. Primary productivity in the sea. P. G. Falkowski. New York, Plenum: 301-319.
- Marra, J., Barber, R.T., Trees, C., Johnson, Z. and Kinkade, C.S. (1996). Primary production and irradiance during an intermonsoon cruise to the Arabian Sea. *Ocean Optics XIII*, Halifax, NS, SPIE.
- Marra, J., C. Langdon and C. Knudson (1995). Primary production, water column changes and the demise of a *Phaeocystis* bloom at the ML-ML site in the northeast Atlantic Ocean. *Journal of Geophysical Research* 100: 6645-6653.
- Marra, J., C. Trees, R.R. Bidigare and R.T. Barber (2000). Pigment absorption and quantum yield in the Arabian Sea. *Deep-Sea Research II* 47: 1279-1299.
- Marra, J., T. Dickey, W.S. Chamberlin, C. Ho, T. Granata, D.A. Kiefer, C. Langdon, R. Smith, K. Baker, R. Bidigare, and M. Hamilton. (1992). The estimation of seasonal primary production from moored optical sensors in the Sargasso Sea. *Journal of Geophysical Research* 97: 7399-7412.
- Marra, J., W.S. Chamberlin, and C. Knudson. (1993). Proportionality between in situ and bio-optical estimates of carbon assimilation in the Gulf of Maine in summer. *Limnology and Oceanography* 38: 231-238.
- Martin, J. H., R. M. Gordon, S.E. Fitzwater (1991) The case for iron. *Limnology and Oceanography* 36, 1793-1802.
- Platt, T., C. L. Gallegos, and W.G. Harrison. (1980). Photoinhibition of photosynthesis in natural assemblages of marine phytoplankton in the Arctic." *Deep-Sea Research* 29: 1159-1170.
- Sosik, H. and B. G. Mitchell (1995). Light absorption by phytoplankton, photosynthetic pigments and detritus in the California Current System. *Deep-Sea Research* 42: 1717-1748.
- Vaillancourt, R. D., J. Marra, R. T. Barber and W. O. Smith. (2003) Primary productivity and in situ quantum yields in the Ross Sea and Pacific sector of the Antarctic Circumpolar Current. *Deep-Sea Research II*, 50 (in press).

## APPENDIX 1: MATLAB code for the algorithm

The following is the MATLAB routine for the productivity algorithm used in PPARR3, and presented in this technical report. It is written as used with the data files provided to PPARR3 participants, although the file loading statements should be easily modified.

---

```
% Global_prod.m
% Calculate global production from global Par, sea surface temperature
% and surface chlorophyll by equation :
%
%   prod=phimax*(Ek/(Ek+E(z)))*ap*chl(z)*E(z)
%
%   gC/m^2/d=12*(molsC/molsPhotons)*(m^2/mg)*(mg/m^3)
%           *(molsPhotons/m^2/d)
%
%
% (cheng Ho, ho@ideo.columbia.edu, 8-1-2002)

% file names for jan, mar, may, july, sept, nov, dec

fnm={'9801.flt';'9803.flt';'9805.flt';'9807.flt';'9809.flt';'9811.flt';'9812.flt'};
ll=length(fnm);

for mm=1:ll
    chl_fnm=['Chl' fnm{mm}];
    par_fnm=['PAR' fnm{mm}];
    sst_fnm=['SST' fnm{mm}];
    prod_fnm=['Prod' fnm{mm}];

% to read the input files

    step=0.087891*2;
    lon=-180:step:180;
    lat=-90:step:90;

    fid=fopen(chl_fnm,'r','ieee-be');
    schl=fread(fid,'float');
    fclose(fid);

    fid=fopen(par_fnm,'r','ieee-be');
    par=fread(fid,'float');
    fclose(fid);
```

```

fid=fopen(sst_fnm,'r','ieee-be');
sst=fread(fid,'float');
fclose(fid);

% from mlml, arabian sea and ross sea data, kc vs sst relationship
% was expressed as:

kc=0.00433*exp(0.08249*sst);

% the exp regression curve did not reflect the actual kc value at southern
ocean. Linear interpolation was introduced.
k4=find(sst<12);
kc(k4)=0.0105+sst(k4)*0.0001;

% kc_p - only part of kc related to productivity, '0.85' is multiplied to
% the 'exp' coefficient.

kc_p=0.00433*exp(0.85*0.08249*sst);

% At lower temperature kc and kc_p should be equal

k4=find(sst<14.475);
kc_p(k4)=0.0105+sst(k4)*0.0001;

% pure water absorption and absorption of 'other':

kw=0.04;kx=0.02;

% max depth : 98m
z=[0:2:98];

% length of global files

len=length(schl);

% to save computer memory, data were divided into 'pages'

% divide the file into 10000 line pages

lim=10000;
page=ceil(len/lim);

```

```

big=lim;

% initialize matrix

chl=zeros(lim,50);
kpar=zeros(lim,50);
E=zeros(lim,50);
prod=zeros(lim,50);
P=zeros(len,1);

pc=0; % percentage done

for jj=1:page

% at the last page, 'page length' is different from 'lim'
    if jj==page,big=len-(page-1)*lim;end

    for kk=1:big
% 'ii' - corresponding location of current data in global data file
        ii=(jj-1)*lim+kk;
        if (ii/len>pc), disp(['now ',num2str(pc*100),'%']), pc=pc+0.1; end

% determine the depth distribution of chlorophyll

        if (schl(ii)>0.4)
            h=42; sig=50; zm=5; y=20;
        else
            h=20; sig=18; zm=75; y=1;
        end
        chl(kk,:)=schl(ii)+(h/sig/sqrt(2*pi))*exp(-(z-zm).^2/2/sig^2)/y;

% calculate the depth distribution of PAR

        kpar(kk,:)=kw+kc(ii)*chl(kk,:)+kx;
%         when kpar not vary too much, this way saves 80% computer time
%         E(kk,:)=par(ii)*exp(-kpar(kk,:).*z);
%         dp=50;

%         This is the correct way
        E(kk,1)=par(ii);
        for i9=2:50
            E(kk,i9)=E(kk,i9-1)*exp(-kpar(kk,i9)*2);
        end
    end
end

```

```

%      find 1% light level depth

      EE=E(kk,:)/par(ii);
      dp=min(find(EE <0.01));

% calculation depth productivity, phimax=0.03

      prod(kk,:)=12*2*0.03*(10./(10+E(kk,:)))*kc_p(ii).*chl(kk,:).*E(kk,:);
% 2: 2 meter steps
% 12: convert to g-mole-C from mmole-mg

      P(ii)=sum(prod(kk,1:dp));

      end
end

% mask out the land area or no-data area

      maxP=50; % possible max for all months is 31
      kkk=find(schl>66.8);P(kkk)=maxP;
      kkk=find(par>76.5);P(kkk)=maxP;
      kkk=isnan(sst);P(kkk)=maxP;

% store data in a file

      fid=fopen(prod_fnm,'w','ieee-be');
      fwrite(fid,P,'float');
      fclose(fid);

% plot the dsta

      F2=reshape(P,2048,1024);
      F3=rot90(F2);
      figure(mm)
      cmap=flipud(hsv);
      cmap(64,:)=0;
      colormap(cmap);
      imagesc(lon,lat,log10(F3)),axis('xy'),colorbar
      hh=colorbar;
      set(hh,'YTick',[log10(0.01) log10(0.03) log10(0.1) log10(0.3) log10(1)
], 'YTickLabel',['0.01'; '0.03'; '0.1'; '0.3'; '1'])

end

```